Discussion Paper No.265

A Heterogeneous Agent Model with Three Delays

Akio Matsumoto
Chuo University

Ferenc Szidarovszky
University of Pécs

May 2016

INSTITUTE OF ECONOMIC RESEARCH
Chuo University
Tokyo, Japan

A Heterogeneous Agent Model with Three Delays*

Akio Matsumoto† Ferenc Szidarovszky‡

Abstract

This paper considers a continuous-time heterogeneous agent model of a financial market with one risky asset, two types of agents (i.e., the fundamentalists and the chartists), and three time delays. The chartist demand is determined through a nonlinear function of the difference between the current price and a weighted moving average of the delayed prices whereas the fundamentalist demand is governed by the difference between the current price and the fundamental value. The asset price dynamics is described by a nonlinear delay differential equation. Two main results are analytically and numerically shown:

(i) the delay destabilizes the market price and generates cyclic oscillations around the equilibrium;

(ii) under multiple delays, stability loss and gain repeatedly occurs as a length of the delay increases.

Keywords: Heterogeneous agents model, Three time delays, Stability switching curves, Delay effect, Bifurcation

*The authors highly appreciate the financial supports from the MEXT-Supported Program for the Strategic Research Foundation at Private Universities 2013-2017, the Japan Society for the Promotion of Science (Grant-in-Aid for Scientific Research (C), 25380238, 26380316 and 16k03556) and Chuo University (Joint Research Grant). The usual disclaimers apply.

†Professor, Department of Economics, Senior Researcher, International Center for further Development of Dynamic Economic Research, Chuo University, 742-1, Higashi-Nakano, Hachioji, Tokyo, 192-0393, Japan; akiom@tamacc.chuo-u.ac.jp

‡Professor, Department of Applied Mathematics, University of Pécs, Ifjúság u. 6., H-7624, Pécs, Hungary; szidarka@gmail.com

1 Introduction

Persistent volatility is a prominent characteristic feature of financial markets. It is, however, well-known that the efficient market hypothesis cannot account for the discrepancy between the observed market price and the fundamental value of the asset. Recently, heterogeneous agent models (HAMs) have been developed to explain a wide variety of financial market behavior such as temporary bubbles, sudden market crashes and price resistance in discrete-time as well as continuous-time framework. In his survey of recent developments of HAMs, Hommes (2006) discusses that nonlinear discrete-time HAMs can generate various dynamics ranging from cyclic fluctuations to chaotic behavior. Among others there is Chiarella et al. (2006) that propose a discrete-time HAM with a moving average (MA) rule having various memory lengths. Their main finding is that the length of the MA rule can be a source of complicated dynamics in destabilized financial markets in deterministic and stochastic processes. On the other hand, continuous-time HAMs are described by ordinary or delay differential equations. They have a long history since Zeeman (1974) and Beja and Goldman (1980). Moreover Chiarella (1992), which is a development of Beja and Goldman (1980), shows that the market price tends to a stable limit cycle under a nonlinear demand function of the risky asset when the equilibrium is unstable. More recently, He and Zheng (2010) reconstruct the discrete-time model of Chiarella et al. (2006) in a continuous-time framework in which the expected price is formed with a moving average of the past (delay) prices. Their main result concerns a *double edge effect* on the stability caused by the length of the memory or delay: an increase in delay can destabilize the market price and also stabilize it. In their model as well as in subsequent studies on continuous-time HAMs such as He and Li (2012) and Xu et al. (2015), it is assumed that infinitely many past price data are available at no charge of cost. Needless to remember the well-known line in economics, "there is no such thing as a free lunch," it is to go too far to get necessary information for nothing. Two ways are possible to render this extreme assumption to more realistic one, the first is to introduce information cost and the second is to limit availability of the past prices. In the present paper, we take the second way and then reconsider the price dynamics when the chartists forecast an expected price, using only a limited information on past prices.

Following the framework of Dibeh (2005), this paper constructs a dynamic HAM of a speculative asset with three delays (i.e., three past prices) and investigates the effect of time delays on the asset price dynamics. Dibeh (2005) conducts mainly with numerical simulations. Analytical developments of a one-delay version and a two-delay version of Dibeh's model are already presented by Qu and Wei (2010) and Matsumoto and Szidarovszky (2015), respectively. The model we analyze is continuation of these preceding studies. One of our main findings is that stability switches from stability to instability as well as from instability to stability can occur in three delay framework. The double edge effect can also exist in continuous-time HAMs with a finite number of delay prices.

The structure of the paper is as follows. Section 2 constructs a HAM model

with the fundamentalists and chartists. The stability switching curve is analytically derived, which divide the delay space into stability and instability regions. Section 3 has three subsections, in each of which we conduct a stability and bifurcation analysis under different circumstances. Section 4 concludes the paper.

2 Model

We consider an asset pricing model with one risky asset and two traders, fundamentalists and chartists. Let $p(t)$ be the price of the risky asset at time t. Since the fundamentalists believe that $p(t)$ eventually converges to ν, the fundamental (i.e., equilibrium) price of the asset, they will sell the asset if $p(t) > \nu$ and buy it if $p(t) < \nu$. The simplest form of the demand function of the fundamentalist is

$$D^f(p(t)) = m\left[\nu - p(t)\right]$$

where $m \in (0,1)$ is the fraction of the fundamentalists in the market. On the other hand, the chartists base their decisions of market participation on the price trend of the asset. Their demand function is

$$D^c(s(t)) = \mu(1-m)g(s(t))$$

where μ is a positive adjustment coefficient and, for analytical simplicity, it is assumed to be unity in the sequel. $s(t)$ is a weighted average of the past price trends formulated at time t,

$$s(t) = \sum_{i=1}^{n} \sigma_i \left[p(t-\tau_{i-1}) - p(t-\tau_i)\right]$$

where $\tau_i \geq 0$ is a time delay with $\tau_0 = 0$ and $\sigma_i \geq 0$ denotes a weight of a price change satisfying $\sum_{i=1}^{n} \sigma_i = 1$. The demand function $g(s)$ is assumed to be hyperbolic tangent as in Chiarella (1992) and Dibeh (2005),

$$g(s) = \tanh(s).$$

The market demand is the sum of demands of the fundamentalists and chartists,

$$D(p(t), s(t)) = D^c(s(t)) + D^f(p(t)).$$

The price dynamics follows Dibeh's formulation in which the growth rate of price is determined by the market demand,

$$\frac{\dot{p}(t)}{p(t)} = D(p(t), s(t))$$

that is written as a nonlinear delay differential equation,

$$\dot{p}(t) = (1-m)p(t)\tanh\left[s(t)\right] + mp(t)\left[v - p(t)\right]. \tag{1}$$

Notice that $s(t)$ can be rewritten as

$$s(t) = \sigma_1 \left[p(t) - \bar{p}_n(t) \right]$$

where

$$\bar{p}_n(t) = \sum_{j=1}^{n} \eta_j p(t - \tau_j)$$

with

$$\eta_j = \frac{\sigma_j - \sigma_{j+1}}{\sigma_1} \text{ for } 1 \leq j \leq n-1 \text{ and } \eta_n = \frac{\sigma_n}{\sigma_1} \left(= 1 - \sum_{j=1}^{n-1} \eta_j \right).$$

Since $\bar{p}_n(t)$ is considered to be the weighted (moving) average of the past n prices, the chartists believe that the price will rise (fall) when the current price is above (below) the average of the n delay prices. If infinitely many price data is available with finite or infinite memory length, the moving average can be presented by continuously distributed time delay such as

$$p_\xi(t) = \int_{t-\xi}^{t} \eta(s) p(s) ds$$

where $0 < \xi \leq \infty$ is the memory length and $\eta(s)$ is a weighting function. This form is used in He and Zheng (2010).

Concerning the specification of $s(t)$, Qu and Wei (2010) examine the case of $n = 1$ in which the trend includes one delay price with $\sigma_1 = 1$

$$s(t) = p(t) - p(t - \tau_1).$$

Matsumoto and Szidarovszky (2015) consider the case of $n = 2$ in which two delay prices are used to formulate the trend,

$$s(t) = \sigma_1 \left(p(t) - p(t - \tau_1) \right) + \sigma_2 \left(p(t - \tau_1) - p(t - \tau_2) \right).$$

or

$$s(t) = \sigma_1 \left\{ p(t) - \left[(1 - \eta) p(t - \tau_1) + \eta p(t - \tau_2) \right] \right\}$$

with

$$\eta = \frac{\sigma_2}{\sigma_1}.$$

With two delay prices, the coefficients are positive and add up to unity in interpolation (i.e., $\sigma_1 > \sigma_2$) whereas one coefficient is negative, the other greater than unity and the sum is unity in extrapolation (i.e., $\sigma_1 < \sigma_2$).

In this study, we move one more step forward and draw attention to the case of $n = 3$ for which the average trend is

$$s(t) = \sigma_1 \left[p(t) - p(t - \tau_1) \right] + \sigma_2 \left[p(t - \tau_1) - p(t - \tau_2) \right] + \sigma_3 \left[p(t - \tau_2) - p(t - \tau_3) \right]$$

or

$$s(t) = \sigma_1 \{p(t) - [\eta_1 p(t-\tau_1) + \eta_2 p(t-\tau_2) + \eta_3 p(t-\tau_3)]\}$$

with

$$\eta_1 = \frac{\sigma_1 - \sigma_2}{\sigma_1},\ \eta_2 = \frac{\sigma_2 - \sigma_3}{\sigma_1} \text{ and } \eta_3 = \frac{\sigma_3}{\sigma_1}.$$

For the sake of convenience, we adopt the following form,

$$s(t) = \sigma_1 p(t) + (\sigma_2 - \sigma_1)p(t-\tau_1) + (1-\sigma_1-2\sigma_2)p(t-\tau_2) - (1-\sigma_1-\sigma_2)p(t-\tau_3).$$

The unique stationary point of dynamic equation (1) is identical with the equilibrium price,

$$p^e = \nu = p(t) = p(t-\tau_j) \text{ for all } t \geq 0 \text{ and } j = 1, 2, 3.$$

It is clear that at the stationary point there is no price trend, $s^e = 0$. Linearizing the nonlinear dynamic equation in a neighborhood of the stationary point yields

$$\dot{p}_\delta(t) = \alpha p_\delta(t) + \beta_1 p_\delta(t-\tau_1) + \beta_2 p_\delta(t-\tau_2) - \beta_3 p_\delta(t-\tau_3) \tag{2}$$

where $p_\delta(t) = p(t) - p^e$ and the coefficients are defined as

$$\alpha = \nu\left[(1-m)\sigma_1 - m\right],$$

$$\beta_1 = \nu(1-m)(\sigma_2 - \sigma_1),$$

$$\beta_2 = \nu(1-m)(1-\sigma_1-2\sigma_2),$$

$$\beta_3 = \nu(1-m)(1-\sigma_1-\sigma_2).$$

With condition $\sum_{i=1}^{3} \sigma_i = 1$, it can be verified that

$$\sigma_3 = 0 \iff \sigma_2 = 1 - \sigma_1,$$

$$\sigma_3 = \sigma_1 \iff \sigma_2 = 1 - 2\sigma_1,$$

$$\sigma_3 = \sigma_2 \iff \sigma_2 = \frac{1}{2}(1-\sigma_1).$$

The locus of $\sigma_3 = 0$ divides the first quadrant of the (σ_1, σ_2) plane into two parts, upper and lower right triangles, and condition $\sigma_3 \geq 0$ eliminates the upper one. The lower triangle is further divided into six subparts by the three loci of $\sigma_2 = \sigma_1$, $\sigma_3 = \sigma_2$ and $\sigma_3 = \sigma_1$. Those divisions are depicted in Figure 1 in which the relations among the magnitudes of σ_1, σ_2 and σ_3 are determined in the following way,

$\sigma_1 > \sigma_2 > \sigma_3$ in region I, $\sigma_3 > \sigma_2 > \sigma_1$ in region IV,

$\sigma_1 > \sigma_3 > \sigma_2$ in region II, $\sigma_2 > \sigma_3 > \sigma_1$ in region V,

$\sigma_3 > \sigma_1 > \sigma_2$ in region III, $\sigma_2 > \sigma_1 > \sigma_3$ in region VI.

Region I is colored in gray as we will limit our analysis to it below. The line of $\sigma_2 = (2-3m)/2(1-m) - \sigma_1$ is shown to be dotted and downward sloping.[1] It is also checked that $\beta_1 = 0$, $\beta_2 = 0$ and $\beta_3 = 0$ hold, respectively, on the loci of $\sigma_2 = \sigma_1$, $\sigma_3 = \sigma_2$ and $\sigma_3 = 0$. On these boundaries the three-delay equation (2) is reduced to one of three two-delay equations, depending on which β_i value becomes zero. Matsumoto and Szidarovszky (2015) consider a two delay equation that corresponds to the one with $\beta_3 = 0$. Their analytical method can be applied to the other two equations as well. In this study, we will confine our attention to the regions in which $\beta_i > 0$.

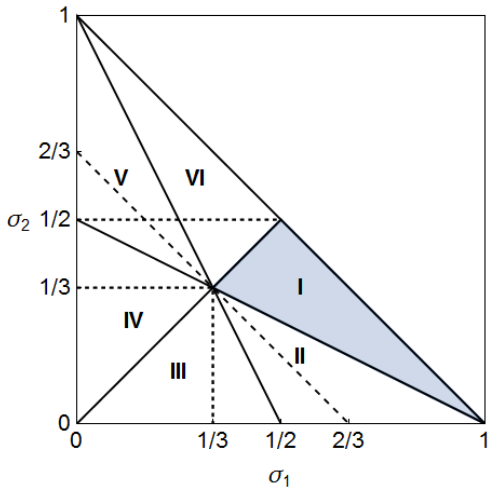

Figure 1. Divisions of the (σ_1, σ_2) plane with $\sigma_3 \geq 0$

Substituting an exponential solution $p_\delta(t) = e^{\lambda t}u$ into the linearized equation (2) yields the corresponding characteristic equation

$$\lambda - \alpha - \beta_1 e^{-\lambda\tau_1} - \beta_2 e^{-\lambda\tau_2} + \beta_3 e^{-\lambda\tau_3} = 0 \tag{3}$$

Dividing the left hand side of equation (3) by $\lambda - \alpha$ and denote the result by $a(\lambda)$,

$$a(\lambda) = 1 + a_1(\lambda)e^{-\lambda\tau_1} + a_2(\lambda)e^{-\lambda\tau_2} + a_3(\lambda)e^{-\lambda\tau_3} \tag{4}$$

with

$$a_1(\lambda) = \frac{-\beta_1}{\lambda - \alpha},\ a_2(\lambda) = \frac{-\beta_2}{\lambda - \alpha},\ a_3(\lambda) = \frac{\beta_3}{\lambda - \alpha}.$$

Since $\lambda = 0$ is not a solution of equation (3), a pair of pure imaginary roots must exist if the stability of the stationary point switches. We thus assume

[1] $m = 0.4$ is assumed and we will refere to this line later.

$\lambda = i\omega,\ \omega > 0$ is a solution of equation (3). For $\lambda = i\omega$,

$$a_1(i\omega) = \frac{\alpha\beta_1 + i\beta_1\omega}{\alpha^2+\omega^2} \text{ and } |a_1(i\omega)| = \frac{|\beta_1|}{\sqrt{\alpha^2+\omega^2}},$$

$$a_2(i\omega) = \frac{\alpha\beta_2 + i\beta_2\omega}{\alpha^2+\omega^2} \text{ and } |a_2(i\omega)| = \frac{|\beta_2|}{\sqrt{\alpha^2+\omega^2}}$$

and

$$a_3(i\omega) = -\frac{\alpha\beta_3 + i\beta_3\omega}{\alpha^2+\omega^2} \text{ and } |a_1(i\omega)| = \frac{\beta_3}{\sqrt{\alpha^2+\omega^2}}.$$

Each term of $a(i\omega)$ may be viewed as a vector in the complex plane. Hence solving $a(i\omega) = 0$ analytically is equivalent to constructing a quadrangle geometrically as shown in Figure 2 in which these four vectors are arranged from head to tail.

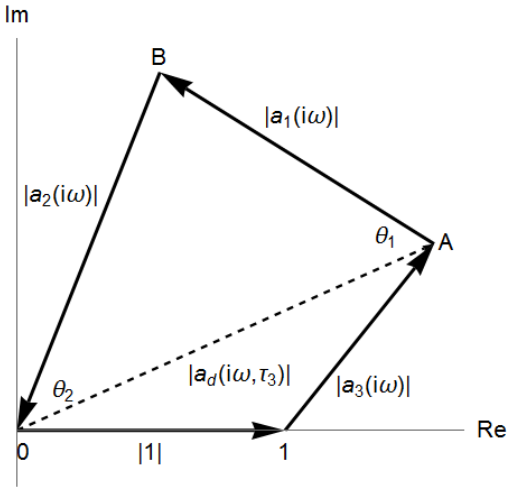

Figure 2. 1 and $|a_j(i\omega)|$ for $j = 1, 2, 3$ forms a quadrangle

The determination of the stability switching surface in the $(\tau_1,\ \tau_2,\ \tau_3)$ plane is challenging.[2] In order to make the problem manageable, we reduce the three-delay equation to a two-delay equation by fixing the value of τ_3 at a certain positive level and then construct the stability switching curve in the (τ_1, τ_2) plane in which we can apply the method used earlier in Matsumoto and Szidarovszky (2015). Notice that vector 1 is connected to vector $a_3(i\omega)e^{-i\omega\tau_3}$ in Figure 2. If the sum of these vectors is denoted by $a_d(i\omega, \tau_3)$,

$$a_d(i\omega, \tau_3) = 1 + a_3(i\omega)e^{-i\omega\tau_3},$$

[2]It is possible to have a switching surface in the 3D space. See Almodaresi and Bozorg (2009) and Gu *et al.* (2011).

then $a(\lambda)$ with $\lambda = i\omega$ can be rewritten as

$$a(i\omega) = a_d(i\omega, \tau_3) + a_1(i\omega)e^{-i\omega\tau_1} + a_2(i\omega)e^{-i\omega\tau_2}.$$

As already shown in Figure 2, $a(i\omega) = 0$ means that these three vectors in $a(i\omega)$ must form a triangle having the dotted base with interior angles, θ_1 and θ_2. Sufficient and necessary conditions for forming a triangle are given by

$$\begin{aligned} &(i)\ f_d(\omega) = |a_1(i\omega)| + |a_2(i\omega)| - |a_d(i\omega, \tau_3)| \geq 0, \\ &(ii)\ f_1(\omega) = |a_2(i\omega)| + |a_d(i\omega, \tau_3)| - |a_1(i\omega)| \geq 0, \\ &(iii)\ f_2(\omega) = |a_d(i\omega, \tau_3)| + |a_1(i\omega)| - |a_2(i\omega)| \geq 0. \end{aligned} \tag{5}$$

Each inequality condition implies that the length of any segment of the triangle is not greater than the sum of the lengths of the remaining two segments. Define the crossing frequency set Ω as all $\omega > 0$ such that $a(i\omega) = 0$ holds for at least one delay combination $(\tau_1, \tau_2, \tau_3) \geq 0$. For $\omega = 0$ in $a(i\omega)$ leads to

$$a(i\omega)|_{\omega=0} = \frac{1}{\alpha}(\alpha + \beta_1 + \beta_2 - \beta_3) < 0.$$

This inequality implies $0 \notin \Omega$.

By the law of cosine, we can determine the values of θ_1 and θ_2 of the triangle in Figure 2,

$$\theta_1(\omega) = \cos^{-1}\left[\frac{|a_d(i\omega, \tau_3)|^2 + |a_1(i\omega)|^2 - |a_2(i\omega)|^2}{2\,|a_d(i\omega, \tau_3)|\,|a_1(i\omega)|}\right]$$

and

$$\theta_2(\omega) = \cos^{-1}\left[\frac{|a_d(i\omega, \tau_3)|^2 + |a_2(i\omega)|^2 - |a_1(i\omega)|^2}{2\,|a_d(i\omega, \tau_3)|\,|a_2(i\omega)|}\right].$$

Vertices A and B maybe located above or below the horizontal axis and the slope of segment AB can be positive or negative. So we have eight possibilities to construct a quadrangle. However, a simple geometric consideration shows that there are only two different possibilities:

$$\arg\left(a_1(i\omega)e^{-i\omega\tau_1}\right) + (2k-1)\pi - \arg(a_d(i\omega, \tau_1)) \pm \theta_1(\omega) = 0$$

and

$$\arg\left(a_2(i\omega)e^{-i\omega\tau_2}\right) + (2n-1)\pi - \arg(a_d(i\omega, \tau_1)) \mp \theta_2(\omega) = 0.$$

Solving these equations for τ_1 and τ_2 yields the threshold values of the delays,

$$\tau_1^{\pm}(\omega, k) = \frac{1}{\omega}\left[\arg(a_1(i\omega) - \arg(a_d(i\omega, \tau_3))) + (2k-1)\pi \pm \theta_1(\omega)\right] \tag{6}$$

and

$$\tau_2^{\mp}(\omega, n) = \frac{1}{\omega}\left[\arg(a_2(i\omega) - \arg(a_d(i\omega, \tau_3))) + (2n-1)\pi \mp \theta_2(\omega)\right]. \tag{7}$$

The stability switching curves consist of two sets of parametric segments,

$$L_1(k,n) = \{\tau_1^+(\omega,k), \tau_2^-(\omega,n)\} \text{ for } k,n = 0,1,2,... \tag{8}$$

and

$$L_2(k,n) = \{\tau_1^-(\omega,k), \tau_2^+(\omega,n)\} \text{ for } k,n = 0,1,2,... \tag{9}$$

where the parameter ω runs through the crossing frequency set Ω.

Substituting $\tau_1 = \tau_2 = \tau_3 = 0$ into equation (3) presents

$$\lambda = \alpha + \beta_1 + \beta_2 - \beta_3 = -\nu m < 0.$$

This inequality implies that the steady state with no delays is stable. Next, assuming that $\tau_1 = \tau_2 = 0$, we examine the existence of a threshold value of τ_3 at which the system loses stability. Without loss of generality, assuming $\lambda = i\omega$, $\omega > 0$ and then substituting it into (3) with $\tau_1 = \tau_2 = 0$ reduce the characteristic equation to

$$i\omega - (\alpha + \beta_1 + \beta_2) + \beta_3 e^{-i\omega\tau_3} = 0.$$

We denote $\alpha + \beta_1 + \beta_2$ by Δ where

$$\Delta = v(1-m)\left(1 - \sigma_1 - \sigma_2 - \frac{m}{1-m}\right)$$

and break down the characteristic equation into the real and imaginary parts,

$$\begin{aligned} -\Delta + \beta_3 \cos\omega\tau_3 &= 0 \\ \omega - \beta_3 \sin\omega\tau_3 &= 0. \end{aligned} \tag{10}$$

Moving Δ and ω to the right hand side and adding the squared equations give

$$\omega^2 = \beta_3^2 - \Delta^2$$

where

$$\beta_3 - \Delta = vm > 0$$

and

$$\beta_3 + \Delta = 2v(1-m)\left(\varphi(\sigma_1) - \sigma_2\right)$$

with

$$\varphi(\sigma_1) = \frac{2-3m}{2(1-m)} - \sigma_1.$$

Notice that the dotted curve in Figure 1 is described by $\sigma_2 = \varphi(\sigma_1)$. It is clear first that

$$\beta_3 + \Delta \gtreqless 0 \text{ according to } \varphi(\sigma_1) \gtreqless \sigma_2$$

and second that

$$\beta_3 + \Delta < 0 \text{ if } m \geq 2/3.$$

This leads to the following result.

Proposition 1 *Given $\tau_1 = \tau_2 = 0$, the solution of delay system (1) is stable for any $\tau_3 \geq 0$ if the fundamentalists dominate over the chartists in the sense that $m \geq 2/3$.*

If $\beta_3 + \Delta > 0$, then there is a ω such as $\bar{\omega} = \sqrt{\beta_3^2 - \Delta^2} > 0$. In this case, loss of stability for $\lambda = i\bar{\omega}$ can be shown in the following way. The characteristic equation with $\tau_1 = \tau_2 = 0$ can be written as

$$\beta_3 e^{-\lambda\tau_3} = \beta_1 + \beta_2 + \alpha - \lambda. \tag{11}$$

Taking λ as a function of τ_3 and differentiating it with respect to τ_3 yield

$$\begin{aligned} \frac{d\lambda}{d\tau_3} &= \frac{\lambda\beta_3 e^{-\lambda\tau_3}}{1 - \tau_3\beta_3 e^{-\lambda\tau_3}} \\ &= \frac{\lambda(\beta_1 + \beta_2 + \alpha - \lambda)}{1 - \tau_3(\beta_1 + \beta_2 + \alpha - \lambda)} \end{aligned}$$

where the right hand side of equation (11) are used. Substituting $\lambda = i\omega$ and taking the real part of the resulting expression give

$$\begin{aligned} \left.\frac{d\left[\operatorname{Re}\lambda\right]}{d\tau_3}\right|_{\lambda=i\omega} &= \operatorname{Re}\left[\frac{\lambda(\beta_1 + \beta_2 + \alpha - \lambda)}{1 - \tau_3(\beta_1 + \beta_2 + \alpha - \lambda)}\right] \\ &= \operatorname{Re}\left[\frac{\omega^2 + i\omega(\beta_1 + \beta_2)}{1 - \tau_3(\beta_1 + \beta_2 + \alpha) - i\omega}\frac{1 + \tau_3(\beta_1 + \beta_2 + \alpha) - i\omega}{1 + \tau_3(\beta_1 + \beta_2 + \alpha) - i\omega}\right] \\ &= \frac{\omega^2}{\left[1 - \tau_3(\beta_1 + \beta_2 + \alpha)\right]^2 + \omega^2} > 0. \end{aligned}$$

This inequality implies that all roots cross the imaginary axis at $i\omega$ from left to right as τ_3 increases so stability is lost. Correspondingly, solving the first equation of (10) for τ_3 presents the threshold value

$$\bar{\tau}_3(\sigma_1, \sigma_2, m) = \frac{1}{\bar{\omega}}\cos^{-1}\left(\frac{\Delta}{\beta_3}\right) > 0 \tag{12}$$

and the system is stable for $\tau_3 < \bar{\tau}_3$ and unstable otherwise.[3] We summarize the results obtained so far.

Proposition 2 *Given $\tau_1 = \tau_2 = 0$, the solution of delay system (1) is stable for $\tau_3 < \bar{\tau}_3(\sigma_1, \sigma_2, m)$, loses stability for $\tau_3 = \bar{\tau}_3(\sigma_1, \sigma_2, m)$ and becomes unstable for all $\tau_3 > \bar{\tau}_3(\sigma_1, \sigma_2, m)$ if the following condition holds,*

$$\sigma_2 < \varphi(\sigma_1)$$

whereas it is always stable for any $\tau_3 > 0$ otherwise.

[3] Solving the second equation of (10) for τ_3 gives the same solution in a different form.

3 Dynamics

Central to this study is the problem of dynamics associated with three fixed delays. This problem is complex and it seems unlikely that an analytical approach to nonlinear delay differential equation (1) would generate fruitful results on dynamics as it might be difficult to solve the equation. In order to understand global dynamics with delays better, it is useful to take a numerical approach. To this end, we make several simplifying assumptions and numerically examine dynamics of the asset price.

Assumption 1. $v = 5,\ m = 0.4$ and $\tau_3 = 5$.

Assumption 2. σ_i for $i = 1, 2, 3$ satisfy $\sigma_1 > \sigma_2 > \sigma_3 > 0$.

Assumption 3. τ_i for $i = 1, 2$ satisfy $\tau_1 < \tau_2 < \tau_3$.

Since the parameter values in Assumption 1 are determined only for computational conveniences, the main results to be obtained below hold for any other values, provided that $m < 2/3$. Assumption 2 implies that the more recent trend has the more weight. This is not necessary but simplifies the analysis. Under $m = 0.4$ of Assumption 1, region I is located above the line $\sigma_2 = \varphi(\sigma_1)$ which is the dotted downward-sloping line passing through point $(1/3, 1/3)$ in Figure 1. Due to Proposition 2, the stationary point is always stable in region I where $\sigma_2 > \varphi(\sigma_1)$ if $\tau_1 = \tau_2 = 0$. Thus it is easy to see how increasing values of these delays affect stability of the steady state. Assumption 3 imposes a natural ordering among the three delays, that is, an older price has a longer delay.

We further divide the region I to determine the ordering among η_i for $i = 1, 2, 3$, the weights of the delay prices to calculate the moving average. Notice that Assumption 2 implies $\eta_i > 0$. By definition, the following equivalent relations hold,

$$\eta_1 \gtreqless \eta_2 \iff \sigma_2 \lesseqgtr \frac{1}{3},$$

$$\eta_2 \gtreqless \eta_3 \iff \sigma_2 \gtreqless \frac{2}{3}(1 - \sigma_1),$$

$$\eta_1 \gtreqless \eta_3 \iff \sigma_1 \gtreqless \frac{1}{2}.$$

Region I is divided into six subdivisions by the loci of $\sigma_2 = 1/3,\ \sigma_2 = 2(1 - \sigma_1)/3$ and $\sigma_1 = 1/2$ and an enlarged part of the divided Region I is depicted in Figure 3. Soon after, we will refer to the black and red dots that we select to

conduct numerical simulations below.

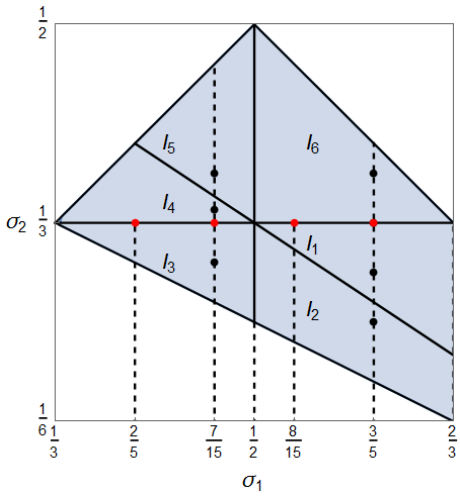

Figure 3. Enlargement of Region I and region division

Accordingly, the following inequality relations hold in the subregions.

$$I_1\colon \eta_1 > \eta_2 > \eta_3, \qquad I_4\colon \eta_3 > \eta_2 > \eta_1,$$

$$I_2\colon \eta_1 > \eta_3 > \eta_2, \qquad I_5\colon \eta_2 > \eta_3 > \eta_1,$$

$$I_3\colon \eta_3 > \eta_1 > \eta_2, \qquad I_6\colon \eta_2 > \eta_1 > \eta_3.$$

The rest of this section has three subsections. We will look at the τ_1-effect on dynamics casued by a change in τ_1 in Section 3.1, explore the τ_2-effect in Section 3.2 and focus on considerations of the τ_3-effect in Section 3.3.

3.1 Delay Effect I: τ_1-effect

We start with the τ_1-effect and present some numerical examples to see how different values of τ_1 affect dynamics of equation (1). We first check the triangle conditions. Subtracting the third equation from the second equation in (5) yields

$$f_1(\omega) - f_2(\omega) = \frac{6\nu(1-m)}{\sqrt{\alpha^2+\omega^2}}\left(\sigma_2 - \frac{1}{3}\right) \tag{13}$$

implying that the relative location of the curves of $f_1(\omega)$ and $f_2(\omega)$ depends on whether a value of σ_2 is larger or less than $1/3$. To simplify the analysis, the value of σ_2 is kept constant at $1/3$ in this subsection, with which $f_1(\omega) = f_2(\omega)$ holds regardless of the value of σ_1. Further $f_i(\omega) > 0$, $i = 1, 2$, for $\omega > 0$

will be numerically confirmed below. Consequently, it is enough to verify only the location and the shapes of the $f_d(\omega)$ curve. We consider dynamics over an interval $[\sigma_1^0, 2/3]$ of σ_1. The left hand side extreme value, $\sigma_1^0 \simeq 0.356$ is numerically determined so as to make the maximum of $f_d(\omega)$ equal to zero. Thus for $\sigma_1 < \sigma_1^0$, $f_d(\omega) < 0$ for all $\omega > 0$, implying that one of the triangle conditions is always violated. The other extreme value, $\sigma_1 = 2/3$, together with $\sigma_2 = 1/3$ makes $\sigma_3 = 0$ via $\sigma_2 = 1 - \sigma_1$. For $\sigma_1 > 2/3$, the nonnegative condition $\sigma_3 \geq 0$ is violated. In the following numerical analysis, σ_1 is increased from 6/15 to 9/15 with an increment of 1/15. Each point is denoted as a red dot along the horizontal line at $\sigma_2 = 1/3$ in Figure 3. The resultant four $f_d(\omega)$ curves are colored in black in Figure 4 where the red curve with $\sigma_1 = 1/2$ and the blue curves with those extreme values are also depicted. The corresponding $f_1(\omega) = f_2(\omega)$ curves are illustrated in the dotted curves with the same color and are seen to be positive for all $\omega \geq 0$. In the gray region below the lower blue curve, no stability switch occurs and thus the steady state is stable. We do not consider the τ_1-effect there. On the other hand, the gray region above the upper blue curve is not feasible and thus eliminated from consideration. Figure 4 illustrates various shapes of the $f_d(\omega)$ curves and shows that increasing σ_1 shifts the curve upward and removes its unevenness. Indeed, the lower blue curve with $\sigma_1 = \sigma_1^0$ located at the bottom of the white region is high-wave shaped while the higher blue curve with $\sigma_1 = 2/3$ at the top is monotonically downward-sloping. In addition, as the red curve passes through the origin, we then see that the curves below the red curve have two intersections with the horizontal axis and the curves above have one intersection.

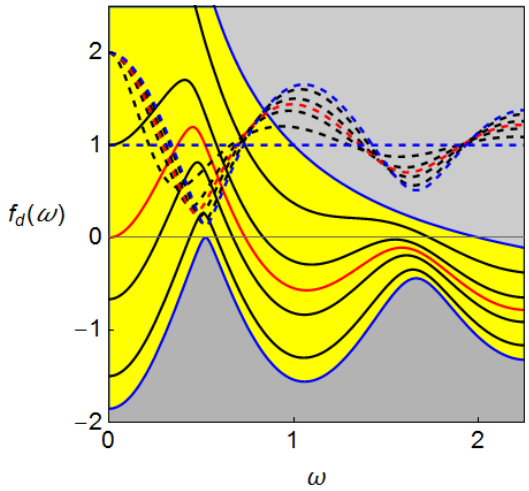

Figure 4. The $f_d(\omega)$ curves with various values of σ_1

To be more specific, we pick up $\sigma_1 = 6/15$ and construct a stability switching

curve. The corresponding $f_d(\omega)$ curve is the black one just above the lower blue curve in Figure 4 and intersects the horizontal axis twice at

$$\bar{\omega}_1 \simeq 0.438 \text{ and } \bar{\omega}_2 \simeq 0.582.$$

The triangle conditions in (5) hold for $\omega \in \Omega = [\bar{\omega}_1, \bar{\omega}_2]$. We now ready to derive the stability switching curves, $L_1(k,n)$ and $L_2(k,n)$ defined in (8) and (9). Taking $k = n = 1$, we obtain the points of $\tau_1^{\pm}(\omega, 1)$ and $\tau_2^{\mp}(\omega, 1)$ by changing values of ω with increment 0.0002 inside the interval $[\bar{\omega}_1, \bar{\omega}_2]$ and then plot these points in the (τ_1, τ_2) plane. In Figure 5(A), segment $L_2(1,1)$ is illustrated as a real curve in the region above the diagonal and segment $L_1(1,1)$ is a dotted curve in the region below.[4] Two segments form an elliptical-shaped closed curve having the starting point $S = (\tau_1^+(\bar{\omega}_1, 1), \tau_2^-(\bar{\omega}_1, 1))$ and the ending point $E = (\tau_1^-(\bar{\omega}_2, 1), \tau_2^+(\bar{\omega}_2, 1))$ on the diagonal where, for $i = 1, 2$,

$$\tau_i^{\pm}(\bar{\omega}_1, 1) = \tau^s \simeq 8.478 \text{ and } \tau_i^{\pm}(\bar{\omega}_2, 1) = \tau^e \simeq 2.789.$$

Since the delays have two constraints, $\tau_i \leq 5$ for $i = 1, 2$ and $\tau_1 < \tau_2$ due to Assumptions 1 and 3, the feasible region should be above the diagonal line and subject to $\tau_2 \leq 5$. It is colored in yellow and further sub-divided into two sub-regions by the $L_2(1,1)$ segment that intersects two lines, one is the diagonal at (τ^e, τ^e) and the other is the horizontal line at $\tau_2 = 5$.[5]

It is clear from the yellow region that stability is preserved for τ_1 and τ_2 such as $0 < \tau_1 < \tau^e$ and $\tau_1 < \tau_2 < \tau^e$. When varying a pair (τ_1, τ_2) with $\tau_2 > \tau^e$ crosses the $L_2(1,1)$ segment, we have the stability switching as the real part of at least one eigenvalue turns to be positive and then the the stationary point loses stability. To see this, we perform a simulation by increasing the value of τ_1 along the dotted horizontal line at $\tau_2 = 4$ that crosses the $L_2(1,1)$ curve at point $(\tau_1^c, 4)$ with $\tau_1^c \simeq 1.640$.[6] The numerical results are summarized in Figure 5(B) in which a bifurcation diagram with respect to τ_1 is depicted. For $\tau_1 \leq \tau_1^c$, a pair of $(\tau_1, 4)$ stays within the stability region. So the stationary point $p^* = v$ is stable and the corresponding part of the bifurcation diagram is a horizontal line at $p(t) = \nu$. Once $\tau_1 > \tau_1^c$, the pair is in the instability region above the $L_2(1,1)$ segment. The stationary point, therefore, loses stability and bifurcates to a limit cycle having two extreme values (i.e., maximum and minimum). The existence of the limit cycle is confirmed by the Hopf bifurcation theorem. Figure 5(B) further implies that the limit cycle becomes larger as τ_1 gets larger and the stability is never regained for $\tau_1 \leq 4$.[7] The τ_1-effect is summarized as follows:

[4] The segment $L_i(k,n)$ shifts upward if n increases and rightward if k increases. For $(k,n) \geq 2$ and $(k,n) = 0$, the switching segments are defined but located ouside of the region with $\tau_i \leq 5$ for $i = 1, 2$, so they are not depicted in Figure 5(A).

[5] The τ_1-value of the intersection is obtained in the following way: first solving $\tau_2^+(\omega, 1) = 5$ for ω yields a solution $\omega_m \simeq 0.560$ and then substituting it into $\tau_1^-(\omega, 1)$ gives $\tau_1^m \simeq 0.887$. So the black segment depicted in the yellow region is defined for $\omega \in [\omega_m, \omega_2]$.

[6] It is possible to obtain this value by following the same procedure with which we obtain the value of τ_1^m just above.

[7] Mathematically, it might be possible to regain stability for $\tau_1 > 4$. However, economically it is not the case as $\tau_1 \leq \tau_2 \leq 5$ is imposed by Assumptions 1 and 3.

Proposition 3 *Stability of dynamic equation (1) with respect to τ_1 depends on the selected value $\bar{\tau}_2$ of τ_2;*

If $\bar{\tau}_2 \leq \tau^e$, then the steady state is stable for $\tau_1 < \bar{\tau}_2$;

If $\bar{\tau}_2 > \tau^e$, then there is the threshold value τ_1^c such that the steady state is stable for $\tau_1 < \tau_1^c$ and loses stability for $\tau_1 \geq \tau_1^c$.

where τ_1^c is the τ_1-point of the intersection of the switching curve and the horizontal line at $\bar{\tau}_2$.

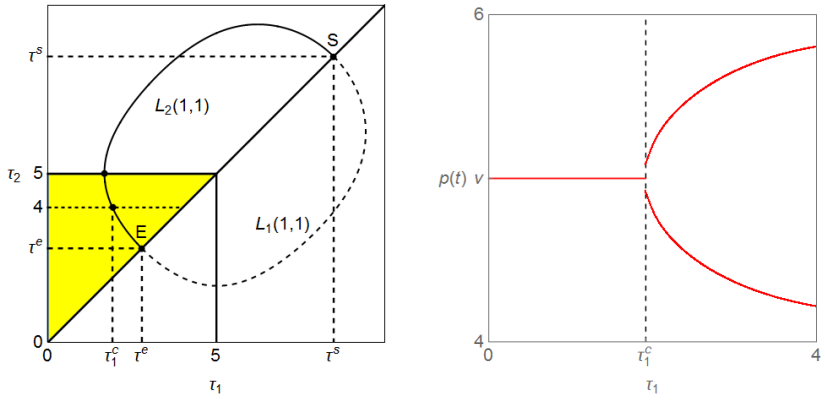

(A) Stability region (B) Bifurcation diagram

Figure 5. Dynamics for $\sigma_1 = 6/15$ and $\sigma_2 = 1/3$

Taking various values of σ_1 out of the interval $[\sigma_1^0, 2/3]$ and constructing the stability switching curves, we detect the τ_1-effect more. In Figure 6(A), the switching curves with various values of σ_1 are illustrated and their end-points on the diagonal are denoted by the red dots. The upper most blue curve has $\sigma_1 = \sigma_1^0$ and the lower most blue curve has $\sigma_1 = 2/3$ while the curve shifts downward as σ_1 increases from σ_1^0 to $2/3$. As far as the curve is single-valued in τ_2, we have essentially the same result on the τ_1-effect as in the case of $\tau_1 = 6/15$: fixing the value of τ_2 at some level and increasing the value of τ_1, the stability is preserved for τ_1 less than the threshold value, τ_1^c and it is lost for $\tau_1 > \tau_1^c$. As seen in Figure 6(A), this threshold value becomes smaller as the value of σ_1 gets larger,[8] a larger value of σ_1 reinforces the destabilizing τ_1-effect.

[8] This is not the case of the non-monotonics curve with $\sigma_1 = 9/15$.

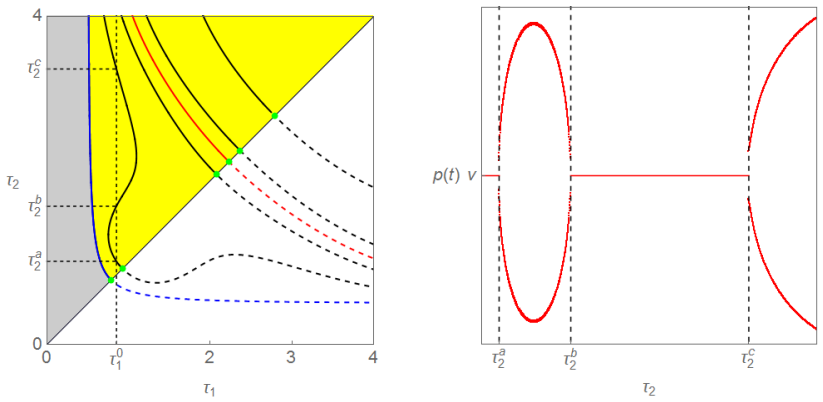

(A) Switching curves (B) Bifurcation diagram

Figure 6. Delay destabilizing and stabilizing effects

3.2 Delay Effect II: τ_2-effect

We are next concerned with the τ_2-effect, how changes in the value of τ_2 affect dynamics. We first return to Figure 5(A) in which both values of σ_1 and σ_2 are fixed. The downward-sloping shape of the switching curve in the yellow region indicates that changing the value of τ_2 with constant τ_1 may generate the similar effect as the τ_1-effect. Let τ_1^m denote the τ_1-value of the intersection of the stability switching curve and the horizontal line at $\tau_2 = 5$.[9] If τ_1 is selected to be less than τ_1^m, then the steady state is stable for any τ_2 that should be above the diagonal and not greater than 5. If $\tau_1^m < \tau_1 < \tau_1^e$, then the steady state is stable for $\tau_2 < \tau_2^c$ and bifurcates to a limit cycle for $\tau_2 > \tau_2^c$ where τ_2^c is defined in the same way as τ_1^c and depends on the value of selected τ_1. One more case exists and is specific to the τ_2-effect, namely, if $\tau_1 > \tau_1^e$, any feasible pair of τ_1 and τ_2 is in the unstable region so that the steady state is unstable.

We now turn attention again to Figure 6(A) and consider the τ_2-effect when σ_1 is increased but σ_2 is still fixed at 1/3. It is already seen that the stationary point is stable in the region left to the stability switching curve and increasing the value of σ_1 shifts the switching curve shifts leftward. The stability switching curve with $\sigma = \sigma_0$ is not depicted as it is located outside Figure 6(A). The shift of the curve implies that a larger value of σ_1 reinforces the destabilizing τ_2-effect in the sense that it makes the stability region smaller. In addition, we have interesting dynamic phenomenon when the switching curve with σ_1 being close to 2/3 has forward- and backward-bending parts. This shape suggests

[9] "τ_1^m" is not labelled in Figure 5(A) to avoid the figure congestion.

the stability loss and gain with respect to τ_2. If the initial point of (τ_1, τ_2) is selected on the diagonal such that the stationary point is stable and the vertical line standing at this value of τ_1 crosses the stability switching curve three times as illustrated in Figure 6(A), then the stability is lost at the first intersection, gained at the second and finally lost again at the third. The corresponding bifurcation diagram is given in Figure 6(B) in which the τ_2 values of the three intersections are denoted as τ_2^a, τ_2^b and τ_2^c, respectively. The increasing delay τ_2 can destabilize the market price, stabilize it and then destabilize it again.

Before analysing the τ_2-effect under various values of σ_2, we assume away $\sigma_2 = 1/3$ and look briefly at a selection of the parameter values of σ_1 and σ_2. According to equation (13), the relative location between the $f_1(\omega)$ and $f_2(\omega)$ curves depends on whether σ_2 is greater or less than $1/3$. It is also observed in Figure 3 that dynamic behavior could be sensitive to the ordering of the weight η_i which is dependent on a combination of σ_1 and σ_2. Thus we examine dynamics more closely in the following six cases where the parameter pair of σ_1 and σ_2 is selected from each of the regions I_i for $i = 1, 2, ..., 6$. In the first three cases we fix $\sigma_1 = 7/15$ and take $\sigma_2 = 3/10$, $\sigma_2 = 31/90$ and $\sigma_2 = 9/24$. These selected points are denoted by the black dots along the vertical line at $\sigma_1 = 7/15$ in Figure 3. Then in the last three cases, we increases the value of σ_1 to $3/5$ and take $\sigma_2 = 6/24$, $\sigma_2 = 7/24$ and $\sigma_2 = 9/24$. These points are also denoted by the black dots on the vertical line at $\sigma_1 = 3/5$.

Case 1: $\sigma_1 = 7/15$ and $\sigma_2 = 3/10$

Notice that this point is in region I_3 in Figure 3. The value of σ_2 being less than $1/3$ leads to $f_1(\omega) > f_2(\omega)$. As is seen in Figure 7(A), the U-shaped blue (i.e., $f_2(\omega)$) curve intersects the horizontal axis twice at

$$\omega_2 \simeq 0.422 \text{ and } \omega_3 \simeq 0.553$$

and the U-shaped green (i.e., $f_1(\omega)$) curve is located far above the horizontal axis, implying that $f_1(\omega) > 0$ for any $\omega > 0$. On the other hand, the unimodal red (i.e., $f_d(\omega)$) curve intersects the horizontal axis also twice at

$$\omega_1 \simeq 0.318 \text{ and } \omega_4 \simeq 0.643.$$

Consequently, the triangle conditions hold in $[\omega_1, \omega_2]$ and $[\omega_3, \omega_4]$ and Ω is a union of these two intervals. The corresponding stability switching curves are obtained by applying equations (8) and (9). However the switching curve defined over $[\omega_1, \omega_2]$ is located outside the feasible region with $0 < \tau_i \leq 5$ for $i = 1, 2$ and $\tau_1 < \tau_2$. Thus only the switching curve defined over $[\omega_3, \omega_4]$ is illustrated as the steepest black curve in the yellow region in Figure 8. As discussed above, the stability is preserved in the region left to the curve whereas it is lost and a limit cycle emerges in the region right to the curve.

Case 2: $\sigma_1 = 7/15$ and $\sigma_2 = 31/90$

This point is in region I_4. Making a value of σ_2 greater than $1/3$ shifts the blue curve upward enough to induce the inequality reversal, $f_1(\omega) < f_2(\omega)$. As is seen in Figure 7(B), both curves are over the horizontal axis and thus $f_1(\omega) > 0$ and $f_2(\omega) > 0$ for any $\omega > 0$. On the other hand, the unimodal red curve intersects it twice at

$$\omega_1 \simeq 0.249 \text{ and } \omega_2 \simeq 0.682.$$

The triangle conditions hold over interval $[\omega_1, \omega_2]$. We can construct the stability switching curve by varying the value of ω from ω_1 to ω_2. It is located to the left to the red curve in the yellow region in Figure 8. Although the detailed derivation is skiped, the red curve denotes the stability switching curve for $\sigma_2 = 1/3$. As in Case 1, the stability is preserved in the region left to the curve whereas it is lost and a limit cycle emerges in the region right to the curve.

Case 3: $\sigma_1 = 7/15$ and $\sigma_2 = 9/24$

This point is in region I_5. It can be seen in Figure 7(C) that an increment of σ_2 shifts the blue curve more upward and the green curve downward enough to intersect the horizontal axis twice. The triangle conditions are fulfilled in the two intervals, $[\omega_1, \omega_2]$ and $[\omega_3, \omega_4]$. By the same reason as in Case 1, only the stability switching curve defined over $[\omega_3, \omega_4]$ is illustrated. It is the flattest black curve in yellow region in Figure 8.

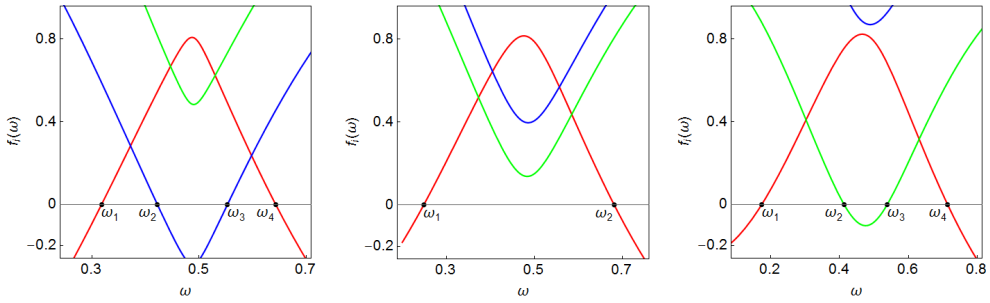

(A) $\sigma_2 = 3/10$ (B) $\sigma_2 = 31/90$ (C) $\sigma_2 = 9/24$

Figure 7. Triangle conditions with $\sigma_1 = 7/15$

As already mentioned, we illustrate four different switching curves in Figure 8, the steepest curve with $\sigma_2 = 3/10$, the red curve with $\sigma_2 = 1/3$, the flatter curve with $\sigma_2 = 31/90$ and the flattest curve with $9/24$. The monotonic shape of the curves implies that dynamics with respect to τ_2 is essentially the same as the one given in Proposition 3.

Proposition 4 *Given σ_1 and σ_2 such as $\sigma_1 < 1/2$ and $(1 - \sigma_1)/2 < \sigma_2 < \sigma_1$, dynamic behavior in regions $I_3 \cup I_4 \cup I_5$ is stable for $\tau_2 < \tau_2^c$ and unstable*

for $\tau_2 > \tau_2^c$ where τ_2^c is the threshold value on the stability switching curve determined by the selected value of τ_1.

Figure 8 also suggests the following effects caused by the change in the value ofparameter σ_2. Decreasing the value of σ_2 from 1/3 to 3/10 moves the red curve to the steeper black curve, affecting the red curve in two steps: it rotates the curve clockwisely around the point on the diagonal in the first step and then shifts the rotated curve downward.[10] Apparently the rotate operation enlarges the stability region and the shift operation contracts it. As far as Figure 8 is concerned in which the shift effect seems very minor, the increase is larger than the decrease. Hence, decreasing the value of σ_2 has a stabilizing effect as it enlarges the stability region. In the same way but in the opposite direction, increasing the value of σ_2 from 1/3 to 31/90 or 9/24 rotates the red curve counter-clockwisely in the first step and then shifts the rotated curve upward in the second step. As a result, the red curves moves to the flatter curve. A decrease of the stability region by the rotate operation is larger than an increase by the shift operation, implying that increasing the value of σ_2 has a destabilizing effect as it enlarges the instability region.

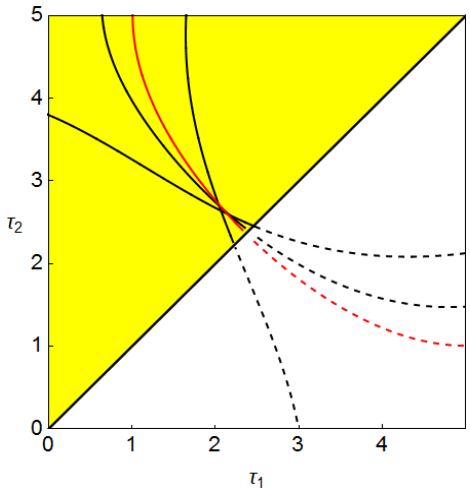

Figure 8. Stability switching curves with $\sigma_1 = 6/15$ and $\sigma_2 = 19/60$, 1/3, 9/24

Case 4: $\sigma_1 = 3/5$ and $\sigma_2 = 6/24$

The point is in I_2. As $\sigma_2 < 1/3$, the blue curve shown in Figure 9(A) is below the green curve and intersects the horizontal axis only once while the red

[10] This decomposition is a hypothetical and intuitive construction in which no mathematical background is provided.

$f_d(\omega)$ curve is strongly convexo-concave and intersects the horizontal axis three times as seen in Figure 9(A). Thus the set Ω is defined as

$$\Omega = [\omega_1, \omega_2] \cup [\omega_3, \omega_4]$$

where

$$\omega_1 \simeq 0.653,\ \omega_2 \simeq 0.904,\ \omega_3 \simeq 1.310 \text{ and } \omega_4 \simeq 1.703.$$

In Figure 10(A), the corresponding stability switching curve is depicted in green and consists of two different segments, one defined over $[\omega_1, \omega_2]$ is downward sloping and the other defined over $[\omega_3, \omega_4]$ is island-shaped. More precisely, the downward sloping curve is described by $L_2(0, 1)$. The green part of the lower island on the right are described by $L_2(0, 1)$ while the green part of the upper island on the left are by $L_1(1, 1)$ and $L_2(1, 1)$. The small part of the island at the upper-right corner is by $L_2(2, 1)$. Since the stationary point is stable in the region left to the downward sloping curve and is outside the island, the τ_2-effect can generate the stability gain as well as the stability loss as will be seen below.

Case 5: $\sigma_1 = 3/5$ and $\sigma_2 = 7/24$

The point is in I_1 and $f_2(\omega) > f_1(\omega)$ still holds as $\sigma_2 < 1/3$. However increasing σ_2 reduces the degree of convexity and concavity of the $f_d(\omega)$ curve. As a result it intersects the horizontal axis only once as shown in Figure 9(A). So the set Ω is identical with $[\omega_1, \omega_2]$ where

$$\omega_1 \simeq 0.526 \text{ and } \omega_2 \simeq 1.717.$$

Increasing the value of σ_2 qualitatively affects the shape of the stability switching curve that is illustrated as the black curve in Figure 10(A). The curve starting on the diagonal first take a round-arch shape and then bends backward to be downward-sloping. Comparing it with the green curves may suggests that increasing the value of σ_2 induces the green downward-sloping curve and the green island-shaped curve to merge to the connected black curve.

Case 6: $\sigma_1 = 3/5$ and $\sigma_2 = 9/24$

We further increase the value of σ_2 to move the point into region I_6. The locations of the blue and green curves are interchanged, $f_2(\omega) > f_1(\omega)$ as shown in Figure 9(C) and $f_2(\omega) > 0$ for all $\omega > 0$. In consequence the green curve and the red curve intersect the horizontal axis once, respectively,

$$\omega_1 \simeq 0.403 \text{ and } \omega_2 \simeq 1.763.$$

The resultant stability switching curve defined over $[\omega_1\ \omega_2]$ is depicted in blue in Figure 10(A).

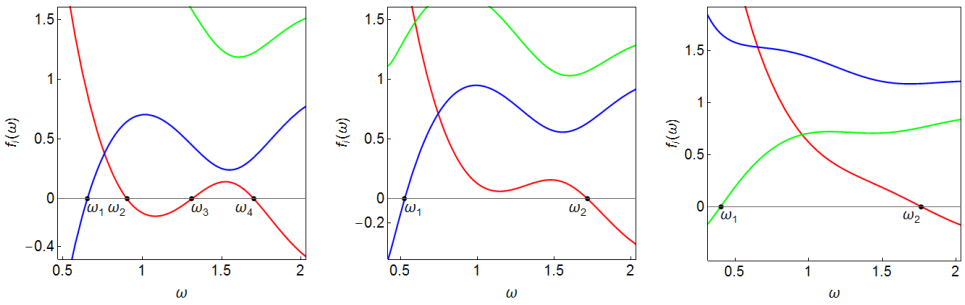

(A) $\sigma_2 = 1/4$ (B) $\sigma_2 = 7/24$ (C) $\sigma_2 = 9/24$

Figure 9. Triangle conditions with $\sigma_1 = 3/5$

In Figure 10(A) there are three (green, black and blue) stability switching curves and the red curve with $\sigma_2 = 1/3$. To see the τ_2-effect, we fix the value of τ_1 at 1.1 and increase the value of σ_2 along the vertical line at $\tau_1 = 1.1$. The line intersects the green and black curves twice, respectively but does not intersect the red curve and the blue curve. As a result, the bifurcation diagrams shown in Figure 10(B) exhibit stability gain and loss for $\sigma_2 = 6/24$ and $\sigma_2 = 7/24$. In particular, along the green curve with $\sigma_2 = 6/24$, the stability is gained at $\tau_2^a \simeq 2.04$ at which the upper and lower branches of the bifurcation diagram merge and lost at $\tau_2^b \simeq 4.282$ at which the horizontal line at $p = \nu$ bifurcates to the upper and lower branches. Similar phenomenon are observed with the black bifurcation diagram for $\sigma_2 = 7/24$. The stability is gained at $\tau_2^A \simeq 1.893$ and lost at $\tau_2^B \simeq 4.444$. The red bifucation diagram exhibits an interesting shape, that is, the difference between the upper and lower branches are sufficiently close for some values of τ_2. This occurs, since the vertical line comes close to but does not intersect the red curve in Figure 10(A)

Proposition 5 *Given σ_1 and σ_2 such as $\sigma_1 > 1/2$ and $(1-\sigma_1)/2 < \sigma_2 < 1-\sigma_2$, new phenomena such as stability loss and gain might occur in region $I_1 \cup I_2 \cup I_6$.*

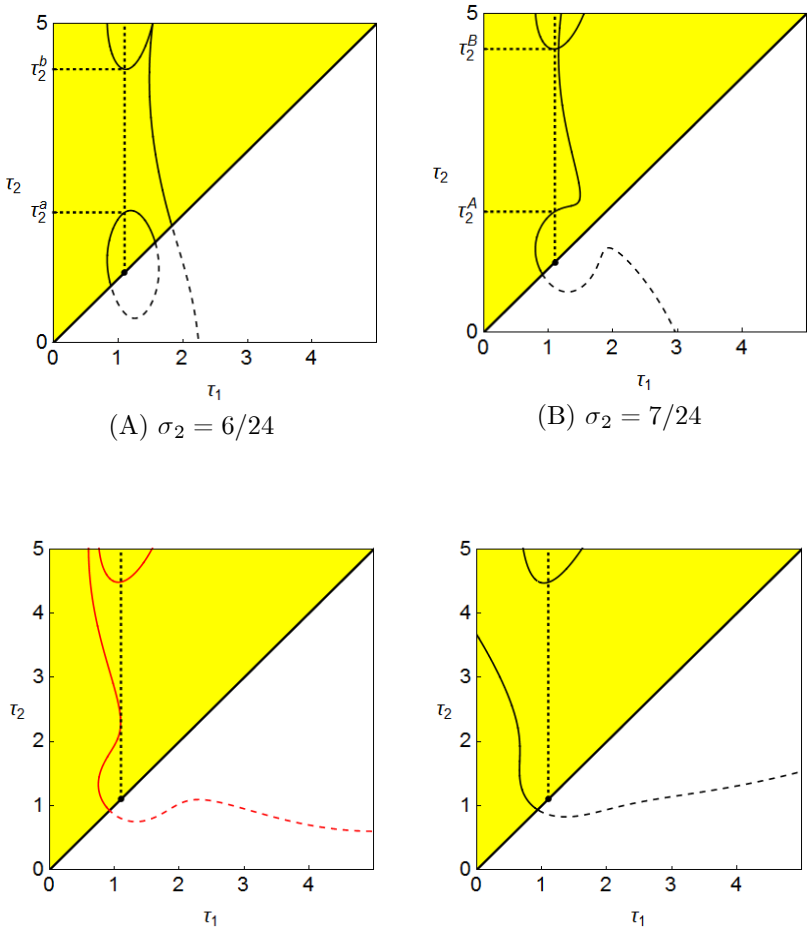

(A) $\sigma_2 = 6/24$ (B) $\sigma_2 = 7/24$

(B) $\sigma_2 = 8/24$ (D) $\sigma_2 = 9/24$

Figure 10. Various stability switching curves

3.3 Delay Effect III: τ_3-effect

We now look into the τ_3-effect, the effect caused by changing the value of τ_3. To this end, $\sigma_1 = (6 - 0.1)/12$ is taken, $\sigma_2 = 1/3$ is re-assumed to simplify the analysis and dynamics with three different values of τ_3, $\tau_3 = 5$, $\tau_3 = 6$ and $\tau_3 = 7$, are considered. The corresponding switching curves are illustrated in different colors in Figure 11(A) (that is, a blue curve with $\tau_3 = 5$, red curves with $\tau_3 = 6$ and black curves with $\tau_3 = 7$). As τ_3 increases, it is observed first that the feasible region of τ_1 and τ_2 increases since the upper bound of τ_2 becomes larger and second that the downward-sloping switching curve shifts upward,

which implies an enlargement of the stability region. It is further observed that island-shaped switching curves emerge for $\tau_3 = 6$ and $\tau_3 = 7$ and the steady state is unstable inside of it. To detect the reason why the island-shaped region is born, we draw the green $f_1(\omega) = f_2(\omega)$ curve and the red $f_d(\omega)$ curve for $\tau_3 = 7$ in Figure 11(B). It is seen that $f_1(\omega) = f_2(\omega) > 0$ for $\omega > 0$ and the larger τ_3 value makes the second hump of the $f_d(\omega)$ curve high enough to cross over the horizontal line. As a result, the red curve intersects the horizontal line four times at

$$\omega_1 \simeq 0.104, \omega_2 \simeq 0.562, \omega_3 \simeq 1.059 \text{ and } \omega_4 \simeq 1.256.$$

In consequence, the triangle conditions (5) hold in the two intervals, $[\omega_1, \omega_2]$ and $[\omega_3, \omega_4]$. It is verified that the switching curve defined on $[\omega_1, \omega_2]$ is downward-sloping and the one on $[\omega_3, \omega_4]$ forms an island shape. The existence of the smaller red islands indicates that the $f_d(\omega)$ curve also intersects the horizontal axis four times even when $\tau_3 = 6$. A critical value of τ_3 for the birth of the island is somewhere between $\tau_3 = 5$ and $\tau_3 = 6$, for which the maximum of the second hump of $f_d(\omega)$ becomes zero.

Proposition 6 *As far as τ_3 is relatively smaller, increasing the value of τ_3 stabilizes the steady state by shifting the switching curve upward whereas for a relatively larger value, increasing value of τ_3 additionally generates an island-shaped switching curve.*

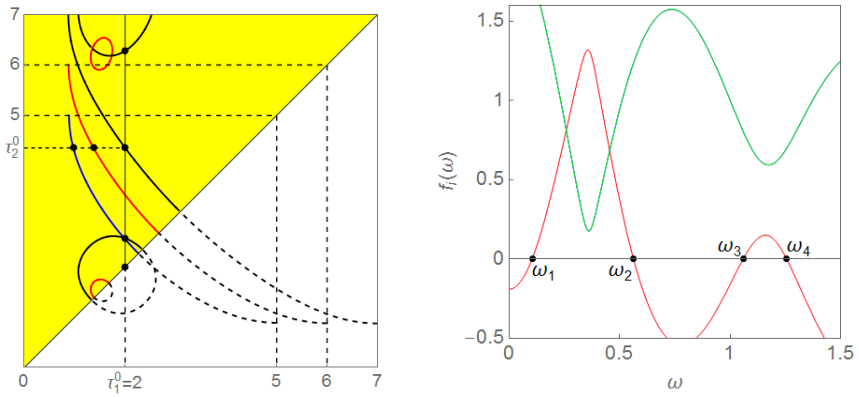

(A) Stability switching curves (B) Triangle conditions

Figure 11. τ_3-effects on switching curves

To see the τ_3-effect on dynamics, we perform two simulations. In the first simulation, we increase the value of τ_1 along the horizontal line at $\tau_2 = \tau_2^0$. This line successively crosses the stability switching curves, the blue curve at $\bar{\tau}_1^c$, the

red curve at $\tilde{\tau}_1^c$ and the black curve at $\hat{\tau}_1^c$ although these bifurcating values are not labelled in Figure 11(A) to avoid confusion. The corresponding bifurcation diagrams are illustrated in Figure 12(A) in which the black curve is depicted first, the red curve is then put on it and finally the blue curve is further placed upon. Each diagram has a qualitatively similar shape as the one in Figure 4(B), that is, the steady state loses stability at the bifurcation value and a limit cycle emerges for a larger value of τ_1. Thus larger τ_3 value does not alter qualitative aspects of the τ_1-effect, however, does affect its quantitative aspects because the bifurcation value of τ_1 becomes larger as τ_3 increases. Increasing value of τ_3 enhances the stabilizing τ_1-effect by delaying the loss of stability.

In the second simulation, we shift the emphasis away from the τ_1-effect to the τ_2-effect and then increase the value of τ_2 from 2 to 7 along the vertical real line at $\tau_1 = 2$ in Figure 11(A), fixing $\tau_3 = 7$ and starting at point $(2, 2)$ on the diagonal. The line crosses the lower black island-shaped curve at τ_2^a, the green downward sloping curve at τ_2^b and then upper circle-shaped curve at τ_2^c. These threshold values are not labelled in Figure 11(A) by the same reason as before. The simulation results are given in Figure 12(B) in which stability gain and loss occur in the following way:

(i) we initially have a unstable steady state (in other words, a stable limit cycle) when the initial point is selected on the diagonal in Figure 11(A)[11] that is inside the half green circle. The real parts of one eigenvalue is positive.

(ii) the limit cycle becomes smaller as τ_2 increases from 2 to τ_2^a and merges with the steady state for $\tau_2 = \tau_2^a$ at which instability is switched to stability. The positive real part turns to be negative when the delay τ_2 crosses the imaginary axis from left to right.

(iii) for $\tau_2^a < \tau_2 < \tau_2^b$, the model has a stable steady state and stability loss occurs for $\tau_2 = \tau_2^b$;. The real parts of at least one eigenvalue turn to be positive again when the delay τ_2 crosses the imaginary axis.

(iv) for $\tau_2 > \tau_2^b$, Figure 12(B) suggests the existence of stable limit cycles and the instability of the steady state. Although increasing τ_2 intersects the island switching curve at point $(2, \tau_2^c)$ at which the real part of another eigenvalue changes sign. However no stability switch occurs, since there is at least one other eigenvalue with positive real part.

Proposition 7 *Changing the value of τ_3 does not affect essentially dynamics with respect to τ_1 and can affect dynamics with respect to τ_2 as it can generate multiple stability switching.*

[11] More precisely, we select a constant initial function, $g(t) = 2$ for $t \leq 0$.

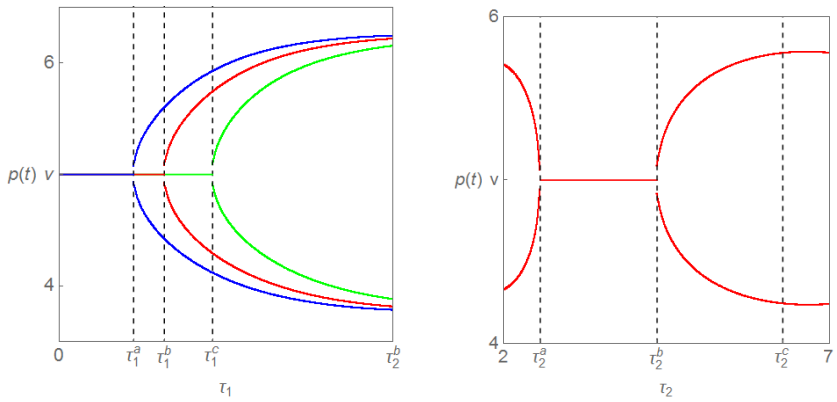

(A) τ_1-effect (B) τ_2-effects

Figure 12. Delay effects on dynamics

4 Concluding Remarks

This paper constructs a heterogeneous agent model with three fixed delays and considers its dynamic behavior both analytically and numerically. The dependence of the delay effects on the changes in the lengths of the delays is also studied. The common result is that a longer delay can destabilize the market and can give rise to cyclic oscillations around the equilibrium (i.e., fundamental) price. This result clarifies the instability condition and thus complements the numerical study of Dibeh (2005). In addition, it is found that under multiple delays, stability loss and gain repeatedly occur as the length of a delay increases. He and Zheng (2010) observed this phenomenon in a financial market model with continuously distributed time delay that involved infinitely many past price observations and called it the double edge effect. It is thus shown that the same effect can occur even under finite delay information. In our future research the model of this paper will be extended to involve two risky assets and the stability and instability of the equilibrium will be examined.

References

[1] Almodaresi, A. and Bozorg, M. Stability Crossing Surfaces for Linear Time-delay Systems with Three Delays, *International Journal of Control*, 82, 2304-2310, 2009.

[2] Beja, A. and Goldman, M. On the Dynamic Behavior of Prices in Disequilibrium, Journal of Finance, 35, 235-248, 1980.

[3] Chiarella, C. The Dynamics of Speculative Behavior, *Annals of Operations Research*, 37, 101-123, 1992.

[4] Chiarella, C., He, X-Z. and Hommes, C. A Dynamic Analysis of Moving Average Rules, *Journal of Economic Dynamics and Control*, 30, 1729-1753, 2006.

[5] Dibeh, G. Speculative Dynamics in a Time-Delay Model of Asset Prices, *Physica A*, 355, 199-208, 2005.

[6] Gu, K., Niculescu, S. and Chen, J. On Stability Crossing Curves for General Systems with Two Delays, *Journal of Mathematical Analysis and Applications*, 311, 231-252, 2005.

[7] Gu, K., Niculescu, S. and Chen, J. On Stability Crossing Set for Systems with Three Delays, *IEEE Transactions on Automatic Control*, 56, 11-26, 2011.

[8] He, X-Z. and Li, K. Heterogeneous Beliefes and Adaptive Behavior in a Continuous-time Asset Price Model, *Journal of Economic Dynamics and Control*, 36, 973-987, 2012.

[9] He, X-Z. and Zheng, M. Dynamics of Moving Average Rules in a Continuous-Time Financial Market Model, *Journal of Economic Behavior and Organization*, 76, 615-634, 2010.

[10] Hommes, C. Heterogeneous Agent Models in Economics and Finance, *Handbook of Computational Economics, Agent-based Computational Economics, II*, North-Holland, 1109-1186, 2006.

[11] Matsumoto, A. and Szidarovszky, F. Heterogeneous Agent Model of Asset Price with Time Delays, *IERCU Discussion Paper #247*, Institute of Economic Research, Chuo University, 2015.

[12] Qu, Y. and Wei, J. Global Hopf Bifurcation Analysis for a Time-Delayed Model of Asset Prices, *Discrete Dynamics in Nature and Society*, 2010, Article ID 432821, DOI:10.1155/2010/432821, 2010.

[13] Xu, X., Liu, J., Guo, L. and Xu, Z. Oscillatory Dynamics in a Continuous-Time Delay Asset Price Model with Dynamical Fundamental Price, *Computational Economics*, 45, 517-529, 2015.

[14] Zeeman. E. On the Unstable Behavior of Stock Exchanges, *Journal of Mathematical Economics*, 1, 39-49, 1974.